*Reproduced with permission; from the authors; Biochem.J. (2000) **346**,385–391. © The Biochemical Society*

Estimation of Systolic and Diastolic Free Intracellular Ca^{2+} by Titration of Ca^{2+} Buffering in the Ferret Heart

Heide L Kirschenlohr, Andrew A Grace, Jamie I Vandenberg, James C Metcalfe and Gerry A Smith[1]

Section of Cardiovascular Biology, Department of Biochemistry, University of Cambridge, Tennis Court Road, Cambridge CB2 1QW, UK. Tel: +44 (0)1223 333632. Fax: +44 (0)1223 333345. Email: g.a.smith@bioc.cam.ac.uk

Spectroscopic Ca^{2+}-indicators are thought to report values of free intracellular Ca^{2+} concentration ($[Ca^{2+}]_i$) that may differ from unperturbed values because they add to the buffering capacity of the tissue. To check this for the heart we have synthesised a new ^{19}F-labelled NMR calcium indicator, 1,2-*bis*-[2-*bis*(carboxymethyl)amino-4,5-difluoro-phenoxy]ethane (4,5FBAPTA) with a low affinity (K_d: 2950nM).The new indicator and four previously described ^{19}F-NMR Ca^{2+} indicators, 1,2-*bis*-[2-*bis*(carboxymethyl)amino-5-fluorophenoxy]ethane (5-FBAPTA), 1,2-*bis*-[2-(1-carboxyethyl)(carboxy-methyl)amino-5-fluorophenoxy]ethane (DiMe-5FBAPTA), 1,2-*bis*-[2-(1-carboxyethyl)(carboxy-methyl)amino-4-fluorophenoxy]ethane (DiMe-4FBAPTA) and 1,2-*bis*-[2-*bis*(carboxymethyl)amino-5-fluoro-4-methylphenoxy]ethane (MFBAPTA), with dissociation constants for Ca^{2+} ranging from 46 to 537nM have been used to measure $[Ca^{2+}]_i$, over the range <100nM to >3μM, in Langendorff-perfused ferret hearts (30°C, pH 7.4, paced at 1.0Hz) by ^{19}F-NMR spectroscopy. Loading hearts with indicators resulted in buffering of the Ca^{2+} transient. The measured end-diastolic and peak-systolic $[Ca^{2+}]_i$ were both positively correlated with indicator K_d The positive correlations between indicator K_d and the measured end-diastolic and peak-systolic $[Ca^{2+}]_i$ were used to estimate the unperturbed end-diastolic and peak-systolic $[Ca^{2+}]_i$ by extrapolation to $K_d = 0$ (diastolic) and to $K_d = \infty$ (systolic) respectively. The extrapolated values in the intact beating heart were 161nM for end-diastolic $[Ca^{2+}]_i$ and 2650nM for peak systolic $[Ca^{2+}]_i$ which agree well with values determined from single cells and muscle strips.

Key words:
Ca^{2+}-transient, NMR spectroscopy, Ca^{2+} indicators, FBAPTA, Cardiac

Introduction

The cardiac free intracellular calcium concentration, $[Ca^{2+}]_i$, has a critical role in determining myofibrillar contraction [1]. Investigation of the role of $[Ca^{2+}]_i$ has been facilitated by the application of luminescent and fluorescent Ca^{2+} indicators which permit accurate and rapid measurements of $[Ca^{2+}]_i$ [2]. These techniques are generally restricted to use in isolated cardiac myocytes or the superficial cells of multicellular preparations [3]. Unfortunately, it is difficult to correlate the contraction of single cardiac myocytes, which are seldom stress-loaded (e.g. [4,5]), or the superficial cells of perfused hearts which may not be representative of heart function as a whole [6], with measures of integrated cardiac contractile function.

The $[Ca^{2+}]_i$ in intact hearts can be measured by ^{19}F-NMR spectroscopy using fluorine-labelled Ca^{2+} chelators ([7–10]). The advantages of this method include the sensitivity of the ^{19}F nucleus by NMR criteria, the absence of endogenous background ^{19}F-NMR signals [11] and the identification of minor cellular cations such as Zn^{2+} bound to the indicator [12]. In addition, NMR spectra may be obtained without motion artefacts due to cardiac contraction [13]. 1,2-*Bis*-[2-*bis*(carboxymethyl)amino-5-fluorophenoxy]ethane (5FBAPTA) has also recently been used to obtain measurements of cardiac $[Ca^{2+}]_i$ *in vivo* [14]. The major disadvantage of the ^{19}F-NMR method is that it requires indicator loading to intracellular concentrations that add significantly to the endogenous

Abbreviations used:
AM, acetoxymethyl ester;
$[Ca^{2+}]_i$, free intracellular Ca^{2+} concentration;
DiMe-5FBAPTA, 1,2-*bis*-[2-(1-carboxyethyl)(carboxymethyl)amino-5fluorophenoxy]ethane;
DiMe-4FBAPTA,1,2-*bis*-[2-(1-carboxyethyl)(carboxymethyl)amino-4-fluorophenoxy]ethane;
5FBAPTA,1,2-*bis*-[2-*bis*(carboxymethyl)amino-5-fluorophenoxy]ethane;
4,5FBAPTA, 1,2-*bis*-[2-*bis*(carboxymethyl)amino-4,5-difluorophenoxy]ethane;
LVDP, leftventricular developed pressure;
MFBAPTA, 1,2-*bis*-[2-*bis*(carboxymethyl)amino-5-fluoro-4-methylphenoxy]ethane;
K_a association constant (affinity)
K_d dissociation constant

[1] *To whom correspondence should be addressed*

cytosolic Ca^{2+}-buffering capacity. This is reflected in perturbations of $[Ca^{2+}]_i$ and a marked decline in left ventricular developed pressure (LVDP) during loading of the indicators ([7–10]). For example, the end-diastolic $[Ca^{2+}]_i$ measured with the prototype ^{19}F-NMR indicator, 5FBAPTA, in the perfused ferret heart paced at 1.0Hz is approximately 500nM [8], which is significantly higher than the unperturbed diastolic $[Ca^{2+}]_i$ which is thought to be in the range 50–200nM (reviewed in [1])**.**

There are currently four ^{19}F-NMR indicators that can be used to measure $[Ca^{2+}]_i$ in intact hearts: 5FBAPTA (K_d: 537nM; [11]), 1,2-*bis*-[2-(1-carboxyethyl)(carboxymethyl) amino-5-fluoro-phenoxy]ethane (DiMe-5-FBAPTA) (K_d: 46nM; [15]), 1,2-*bis*-[2-(1-carboxyethyl) (carboxymethyl)amino-4-fluorophenoxy]ethane (DiMe-4FBAPTA) (K_d: 155nM; [15]) and 1,2-*bis*-[2-*bis* (carboxymethyl) amino-5-fluoro-4-methylphenoxy] ethane (MFBAPTA) (K_d: 270nM; [16]).

We have previously shown that the observed $[Ca^{2+}]_i$ in the Langendorff-perfused ferret heart was significantly lower when measured with the high-affinity indicator DiMe-5FBAPTA than with 5FBAPTA [17]. However, when both DiMe-5FBATPA and 5FBAPTA were loaded sequentially, into the same heart, the end-diastolic $[Ca^{2+}]_i$ appeared to be determined mainly by the indicator with the lower affinity [17], although the evidence was indirect as the two indicators used could not be resolved spectroscopically. Nevertheless, the data suggest that the buffering properties of the Ca^{2+} indicators can significantly modify $[Ca^{2+}]_i$.

In the present study we have used a new low-affinity Ca^{2+}-indicator, 1,2-*bis*-[2-*bis*(carboxymethyl)amino-4,5 -difluorophenoxy]ethane (4,5FBAPTA) (K_d:2950nM), together with the indicators previously synthesised in our laboratory (5FBAPTA, DiMe-4FBAPTA and DiMe-5FBAPTA, see above), as well as MFBAPTA [16], to measure end-diastolic $[Ca^{2+}]_i$ and peak-systolic $[Ca^{2+}]_i$. The aim was to determine the relationship between the Ca^{2+} affinity of an indicator and the perturbations of apparent end-diastolic $[Ca^{2+}]_i$ and peak-systolic $[Ca^{2+}]_i$, and to determine whether we could estimate the unperturbed diastolic and systolic $[Ca^{2+}]_i$ in the intact beating heart by extrapolation to zero affinity and infinite affinity respectively.

Materials and Methods

Synthesis of 4,5FBAPTA

The new indicator, 4,5FBAPTA, was synthesised from 3,4-difluorophenol by similar methods to those described [11,15]. In brief, 3,4-difluorophenol was nitrated with concentrated nitric acid in glacial acetic acid at 5°C until completion (assayed by thin layer chromatography on silica developed in chloroform). The reaction mixture was then diluted with water and the crude product isolated by extraction into petroleum spirit. Pure 2-nitro-4,5-difluorophenol was isolated as a gum from the more polar minor product, 2-nitro-3,4-difluorophenol, by silica gel chromatography in petroleum spirit. Condensation with 1,2-dibromoethane in dimethylformamide, with sodium carbonate, yielded the *bis*(4,5-difluoro-2-nitrophenoxy)ethane which was precipitated with water and isolated by filtration (MP 138–141°C).

The dinitro compound was reduced in ethanol, with hydrogen, over palladium on charcoal, and the diamine was recovered by filtration and evaporation. Alkylation of the diamine with methyl bromoacetate, in acetonitrile and diisopropylethylamine, gave the tetramethyl ester of 4,5FBAPTA which was isolated by partitioning into toluene with ammonium phosphate (1M, pH 3) and purified by silica gel column chromatography (ethyl acetate/toluene gradient) and crystallisation from diethyl ether (MP 118–120°C). The free acid was obtained by hydrolysis with excess sodium hydroxide in ethanol followed by dilution with water, acidification with HCl at 5°C and filtration. The preparation of the tetra-acetoxymethyl ester followed the standard procedure [18].

K_d measurements

The Ca^{2+}-affinity of 4,5FBAPTA was measured by titration at 200–400nm in 30mM potassium citrate buffered to pH 7.2 with 40mM HEPES at 30°C. Varying proportions of two 10μM solutions of indicator, one without added Ca^{2+} and the other with a saturating concentration of $CaCl_2$ (20mM, pH corrected to 7.2), were mixed to determine affinities. The K_d at 30°C was confirmed by direct titration at 200–400nm in a 5cm cuvette of a 1μM indicator solution with 1mM $CaCl_2$ in 100mM KCl, 20mM HEPES without a Ca^{2+} buffer. EGTA (1mM) was added to a separate sample to determine the zero $[Ca^{2+}]$ spectrum. The basal $[Ca^{2+}]$ and affinity were calculated by iteration [15]. Finally, K_d was also determined by measuring the areas of bound and free NMR signals for various Ca^{2+} concentrations using 100μM indicator in citrate buffer [15]. All calculations of affinities were iterative and took account of free, bound and basal Ca^{2+} concentrations. For all K_d determinations the slopes of the log([bound indicator]/[free indicator]) against log$[Ca^{2+}]$ plots were 1.0 ± 0.02. The affinities of hydrolysed samples of acetoxymethyl esters of all the indicators used in this study were the same as for

the free acids of the indicators. The addition of up to 1% w/v BSA did not affect indicator K_d suggesting that any interactions with the protein did not affect the Ca^{2+}-affinity of the indicators. The affinities for a series of heavy metals were also measured by UV titration in citrate buffer using the published affinities of the heavy metals for citrate [19,20].

Heart perfusion

Hearts were prepared as previously described [21,22]. In brief, male ferrets (approx. 6 months old) weighing <1.5kg were anaesthetised with sodium pentobarbitone (250mgkg^{-1} intraperitoneally) (May and Baker Limited, Dagenham, Essex, UK) and heparinised (2000i.u. intraperitoneally) (Sigma Chemicals, Poole, Dorset, UK). Hearts were rapidly excised, weighed and arrested in ice-cold perfusion solution (see below). The aorta was cannulated and the heart Langendorff-perfused at a constant flow rate of 4ml min^{-1} (g wet wt)$^{-1}$ with a Krebs-Henseleit buffer containing (in mM) 119 NaCl, 4 KCl, 1.8 $CaCl_2$, 1 $MgCl_2$, 25 $NaHCO_3$, 10 glucose and 5 sodium pyruvate, equilibrated to pH 7.4 with 95% O_2–5% CO_2, and maintained at 30°C.

The atrio-ventricular node was crushed and the heart paced using square-wave stimuli of 10ms duration (Grass S48 Stimulator; Grass Instruments Company, Quincy, MA, USA) at twice threshold voltage at a rate of 1.0Hz controlled by the spectrometer [8]. Pacing electrodes were connected to the heart via salt bridges (polythene tubing, ID=1.1mm, filled with agar saturated with 3M NaCl) and placed in the right ventricular cavity. LVDP was measured using a fluid-filled latex balloon inserted into the left ventricular cavity connected to a pressure transducer (Spectramed P23XL; Spectramed, Inc., Oxnard, California, USA). The balloon volume was adjusted to achieve an initial end-diastolic pressure of 10–20mmHg (1mmHg=133.3 Pa). Stimulus pulse, aortic perfusion pressure, and LVDP were recorded on a 4-channel chart recorder (Gould 2400S; Gould Electronics Limited, Hainault, Essex, UK.) and tape recorder (Racal, model 4S, Southampton, UK).

The heart was allowed to equilibrate for approx. 90min, after which the perfusion pressure was routinely 70–80mmHg. After this period, hearts with a systolic LVP of less than 110mmHg were rejected. The peak-systolic pressure (means±S.D.) in the hearts used was 149±6.0mmHg at an end-diastolic pressure of 15±1mmHg (n=18). At the end of each experiment the hearts were blotted dry and weighed (mean heart weight=7.9±0.3g; n=18). Decline in LVDP was <15% over 5 hours.

Indicator loading

The ^{19}F-NMR indicators were loaded as cell-permeable acetoxymethyl ester (AM) derivatives. All indicators were made up as 50mM stock solutions in DMSO. Indicators were loaded into the hearts at a constant rate of 250μl/h by infusion into the lines carrying the perfusate via a syringe pump, downstream of the bubble trap and filter systems. The perfusate was not re-circulated either during the loading or the following 40min. Loading was stopped when adequate signal to noise (S/N) ratios (>10:1) were achieved.

The hydrolysis rates by endogenous esterases of the acetoxymethyl esters of the five indicators varied and determined the time required for indicator loading. Loading was most rapid for 5FBAPTA-AM with an adequate S/N ratio for the spectrum of 5FBAPTA obtained after 30min loading. The other four indicators were hydrolysed more slowly. To increase the rate of hydrolysis, these indicators were mixed in a 2:1 (v/v) ratio with 25% (w/w) Pluronic F-127 (BASF, Ludwigshafen, Germany) in DMSO before injection into the perfusion line [9,17]. Pluronic F-127 is a non-ionic dispersing agent which helps to solubilise large dye molecules in physiological media [23]. Using this mixture, the loading times were 110min for 4,5FBAPTA-AM and MFBAPTA-AM, 80min for DiMe-5FBAPTA-AM and 70min for DiMe-4FBAPTA-AM. The addition of Pluronic F-127 on loading indicators into hearts had no significant effect on LVDP or end-diastolic $[Ca^{2+}]_i$, although end-diastolic pressure was slightly higher (<5 mmHg) when Pluronic F-127 was omitted during loading [17].

Hearts were allowed to equilibrate for 40mins following loading of indicators, before the acquisition of data. The concentration of indicator in the cytosolic space is proportional to the area of the ^{19}F-NMR resonances of the indicator and, in a previous report, using ^{3}H-labelled 5FBAPTA, we showed that, at a S/N ratio of 10/1, the intracellular concentration of 5FBAPTA was 120μM [21]. All indicators were loaded to similar S/N levels and it was assumed that the final cytosolic concentration of each of the indicators reached approximately 120μM.

Consecutive loading of indicators

For simultaneous $[Ca^{2+}]_i$ measurements by two indicators, hearts were loaded sequentially with two indicators of different K_d but overlapping titration ranges. In one set of experiments MFBAPTA was loaded for 110min followed by a 40min equilibration period and subsequent data collection. Thereafter, the lower affinity indicator, 5FBAPTA, was loaded for 30min followed by a 40min equilibration period and data collection was repeated. In a second set of experiments, DiMe-4FBAPTA was loaded for 70min plus a 40min equilibration period followed by perfusion with the high-affinity indicator, DiMe-5FBAPTA, for 80min plus 40mins equilibration before NMR measurements were made.

NMR measurements

Hearts were placed in a 9.4 Tesla, 89mm bore Bruker AM 400 NMR spectrometer, operating at 376MHz for ^{19}F and equipped with a purpose-built 33mm diameter probehead as described previously [8]. The magnet was shimmed using the perfusate proton signal: ^{1}H line widths at half-height of <60Hz were routinely obtained. End-diastolic $[Ca^{2+}]_i$ and the Ca^{2+} transients were obtained using gated pulse sequences described previously [8,21].

$[Ca^{2+}]_i$ measurements by NMR

The concentration of Ca^{2+}-bound indicator [bound] and free indicator [free] are proportional to the area under their respective resonance peaks. The areas under the bound and free resonances were determined by cutting and weighing [8]. $[Ca^{2+}]_i$ measured by each indicator corresponds to the observed signal intensities according to the following equation: $[Ca^{2+}]_i = K_d \times [bound]/[free]$. All values are reported as means ± SD.

Results

K_d measurements

The K_d values for the indicators measured at 30°C by UV spectroscopy are shown in Table 1. All values were confirmed using NMR spectroscopy and lay within the range ±5% of the values shown in Table 1. Our value for the K_d of MFBAPTA at 30°C (220nM, using esterase hydrolysed AM ester) is consistent with the 270nM measured at 37°C by Levy *et al.* (1987). The ^{19}F-calcium indicators are polyvalent cation chelators and if the ion being chelated is non-paramagnetic the fluoroBAPTAs show unique cation-induced chemical shifts. Where the affinity and the concentration of a cation are appropriate the fluoroBAPTA will function as an indicator for that cation, for example, 5FBAPTA has been used to measure Pb^{2+} [24] and Zn^{2+} [12] in biological tissue. Most importantly for the purposes of this study, the indicators retained selectivity for Ca^{2+} relative to other cations (e.g. DiMe-5FBAPTA: $K_{Ca}/K_{Mg} \approx 10^{-6}$, see Table 2).

Indicator	K_d 30°C (nM)	Titration range (nM)	Loading time (min)	End-diastolic $[Ca^{2+}]_i$ (nM)	n	Systolic $[Ca^{2+}]_i$ (nM)	n	dLVP (% of initial)
4,5FBAPTA	2950	520–17000	110	604±29	3	2512±210	2	30±4
5FBAPTA	537	100–3000	30	522±54	12	1871±123	3	23±2
MFBAPTA	220	40–1100	110	342± 24	3	nd	-	18±3
DiMe-4FBAPTA	155	30–900	70	265±26	4	706±75	5	9±4
DiMe-5FBAPTA	46	8–300	80	177±21	14	out of range	-	10±2

Table 1: Ca^{2+} binding properties of ^{19}F-NMR Ca^{2+} indicators

Indicator	Characteristic	Ca^{2+}	Mg^{2+}	H^{+}	Sr^{2+}	Ba^{2+}	Ni^{2+}	Fe^{2+}	Co^{2+}	Mn^{2+}	Zn^{2+}	Cu^{2+}	Cd^{2+}	La^{3+}
5FBAPTA														
	logK_a			5.85	5.26	5.96	6.88	8.1	8.59	8.76	8.89	12.83	12.96	10.06
	Shift (ppm)	5.6			4.7	3.7	32.6	27.1	31.7	broad	3.6	broad	4.9	6.3
DiMe-5FBAPTA														
	logK_a	7.33	1.94	6.5				7.8			8.6			9.96
	shift1 (ppm)	3.96		10.5				16			6.05		3.06	4.58
	shift2 (ppm)							6					3.34	5.6
	shift3 (ppm)													5.75

Table 2: Further biophysical characteristics of the indicators

NMR chemical shifts

The new indicator, 4,5FBAPTA (Figure 1A), showed two resonances from the Ca^{2+}-bound indicator, which were approx. 2ppm and 7ppm downfield from the single peak, corresponding to the two overlapping resonances of the free indicator (Figure 1B). The Ca^{2+}-induced shifts were similar to the shifts of the single fluorine resonances from 4FBAPTA and 5FBAPTA, although the whole spectrum is shifted approximately 26ppm upfield. NMR spectra for the other indicators have been published previously [11,15,16]. The chemical shifts of the free and bound resonances for all the indicators used are shown in Figure 2.

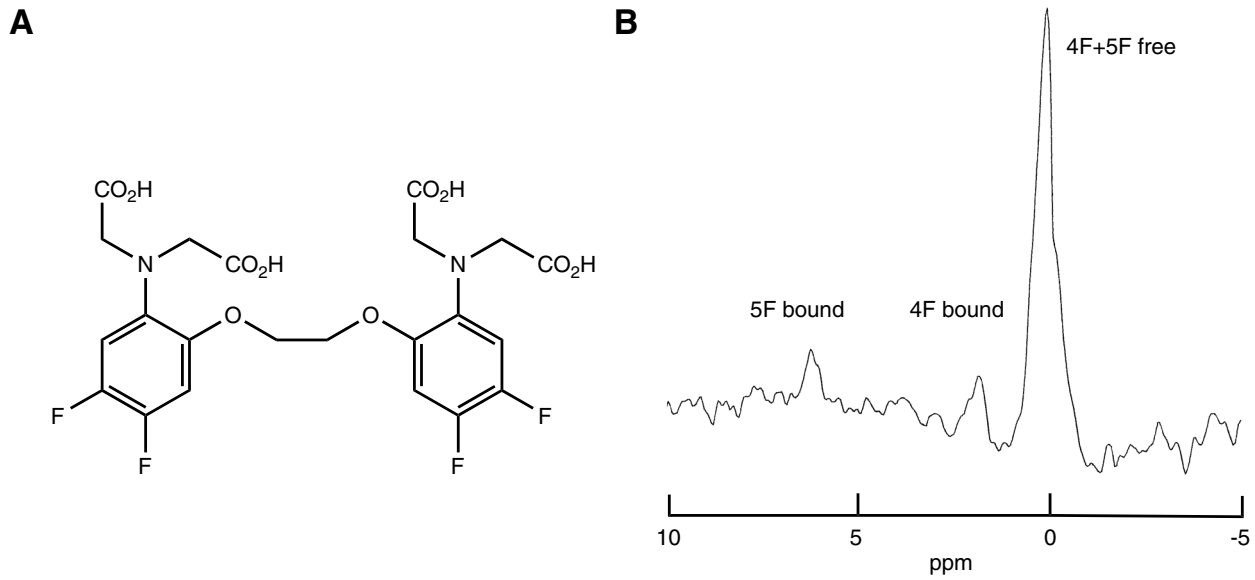

Figure 1: Properties of the new ^{19}F-NMR Ca^{2+} indicator 4,5FBAPTA

(A) The structure of 4,5FBAPTA **(B)** ^{19}F-NMR spectrum obtained at end-diastole from a Ferret heart, paced at 1.0Hz at 30°C, loaded with 4,5FBAPTA (see Methods). The ratio of the Ca^{2+}-bound to free 4,5FBAPTA resonance was 0.17 which represents a $[Ca^{2+}]_i$ of 518nM.

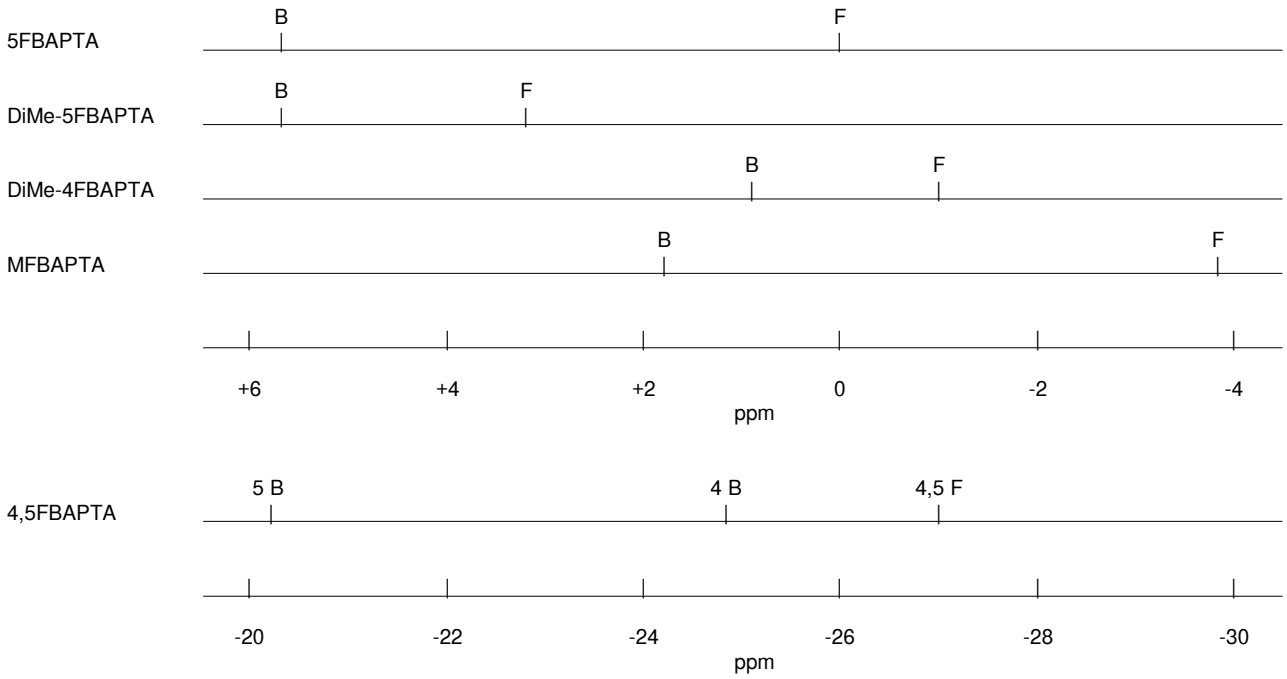

Figure 2: Diagram illustrating the ^{19}F-NMR chemical shifts of the Ca^{2+} indicators loaded into the Ferret heart

All the indicators used in this study are in slow NMR exchange with Ca^{2+} at 376MHz. Chemical shifts are expressed relative to value of 0ppm assigned to the resonance of free 5FBAPTA.

Relationship between indicator K_d, LVDP and $[Ca^{2+}]_i$

When hearts were loaded with the new indicator, 4,5FBAPTA, there was a marked decrease in peak-systolic pressure and a small increase in end-diastolic pressure. By the time adequate S/N ratios were achieved (>10/1) LVDP had decreased to 30% of the pre-loading LVDP (see Table 1). The end-diastolic $[Ca^{2+}]_i$ measured in hearts loaded with 4,5FBAPTA and paced at 1.0Hz, was 604±29nM (n=3) and peak-systolic $[Ca^{2+}]_i$ was 2512±210nM. The corresponding $[Ca^{2+}]_i$, and residual LVDP after loading each indicator are summarised in Table 1.

The end-diastolic $[Ca^{2+}]_i$ increased by more than 3-fold when indicator K_d increased by 60-fold, from 177±21nM (n=14) when measured with DiMe-5FBAPTA to 604±29nM (n=3) when measured with 4,5FBAPTA (Figure 3A). For the four higher affinity indicators (DiMe-5FBAPTA, DiMe-4FBAPTA, MFBAPTA and 5FBAPTA) the diastolic $[Ca^{2+}]_i$ measured with each indicator was approximately linearly related to the indicator K_d.

Extrapolation of these values to an indicator with zero K_d gives an estimated diastolic $[Ca^{2+}]_i$ of 161nM. The systolic $[Ca^{2+}]_i$, measured with the lower affinity indicators, DiMe-4FBAPTA, 5FBAPTA, and 4,5FBAPTA also showed a positive correlation with indicator K_d (Figure 3B). It was not possible to measure the systolic $[Ca^{2+}]_i$ in hearts loaded with DiMe-5FBAPTA, as at $[Ca^{2+}]_i$ >400nM, the area of the free peak was too small to be distinguished from noise. The plot of systolic $[Ca^{2+}]_i$ against indicator affinity is pseudo-exponential and as the affinity approaches zero the value of the systolic $[Ca^{2+}]_i$ approaches 2650nM (broken line, Figure 3B).

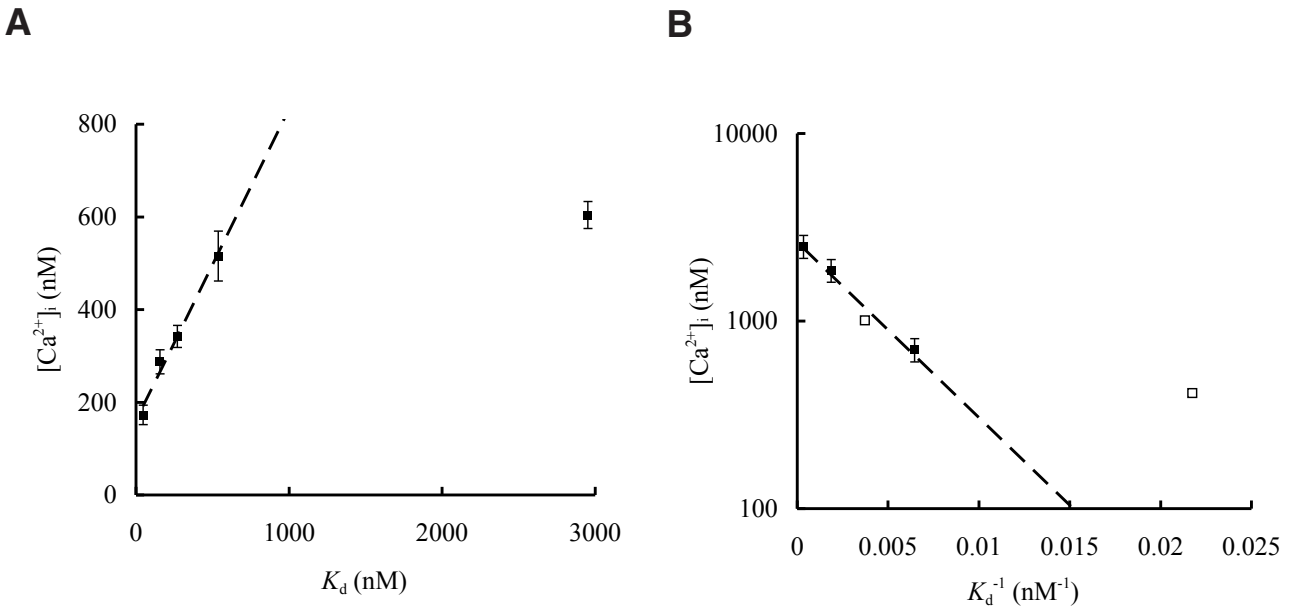

Figure 3: Correlations between indicator K_d and diastolic and systolic $[Ca^{2+}]_i$

(A) End-diastolic $[Ca^{2+}]_i$ plotted against the dissociation constant (K_d) of the indicator used for the $[Ca2+]_i$ measurement. The broken line represents the linear extrapolation used to estimate the unperturbed end-diastolic $[Ca^{2+}]_i$ (see text for details). **(B)** Peak-systolic $[Ca^{2+}]_i$ plotted against the affinity ($1/K_d$) of the indicator used for the measurement. The dashed line represents the log-linear extrapolation used to estimate the unperturbed peak-systolic $[Ca^{2+}]_i$ (see text for details). The open symbols represent values for peak systolic $[Ca^{2+}]_i$ estimated from cytosolic buffering in the presence of MFBAPTA and DiMe5FBAPTA as these values could not be measured experimentally. These estimated values were not used in the extrapolations to obtain the unperturbed systolic $[Ca^{2+}]_i$.

Effect of indicator co-loading on end-diastolic $[Ca^{2+}]_i$

Effective co-loading experiments require indicators whose free and Ca^{2+}-bound resonances do not coincide but whose titration ranges overlap sufficiently to enable accurate $[Ca^{2+}]_i$ measurements with both indicators [16,17]. From the ^{19}F-NMR chemical shifts of the five indicators loaded in perfused ferret hearts (Figure 2) and the K_d values in Table 1, the indicator pairs: 5FBAPTA with MFBAPTA and DiMe-5FBAPTA with DiMe-4FBAPTA, were selected as suitable for co-loading experiments (see Figure 4).

In the first set of experiments MFBAPTA was loaded before 5FBAPTA (Figure 4A). MFBAPTA alone gave an end-diastolic $[Ca^{2+}]_i$

of 327±24nM (n=3), but after the loading 5FBAPTA into the same heart, the end-diastolic $[Ca^{2+}]_i$ increased significantly to 439±15nM, measured with MFBAPTA, or 534±31nM (n=3), measured with 5FBAPTA. The latter value is comparable to the end-diastolic value of 522±54nM (n=12) measured in hearts loaded with 5FBAPTA alone. In the second series of experiments DiMe-4FBAPTA was loaded before DiMe-5FBAPTA (Figure 4B).

DiMe-4FBAPTA alone reported an end-diastolic $[Ca^{2+}]_i$ value of 265±45nM (n=4). Loading DiMe-5FBAPTA into the same heart did not change the end-diastolic $[Ca^{2+}]_i$ measured with DiMe-4FBAPTA, i.e. 275±40nM. The end-diastolic $[Ca^{2+}]_i$ measured with DiMe-5FBAPTA was 204±32nM (n=4, $p < 0.05$ compared to the value measured in hearts loaded with DiMe-5FBAPTA alone, i.e. 171±21nM, n=9).

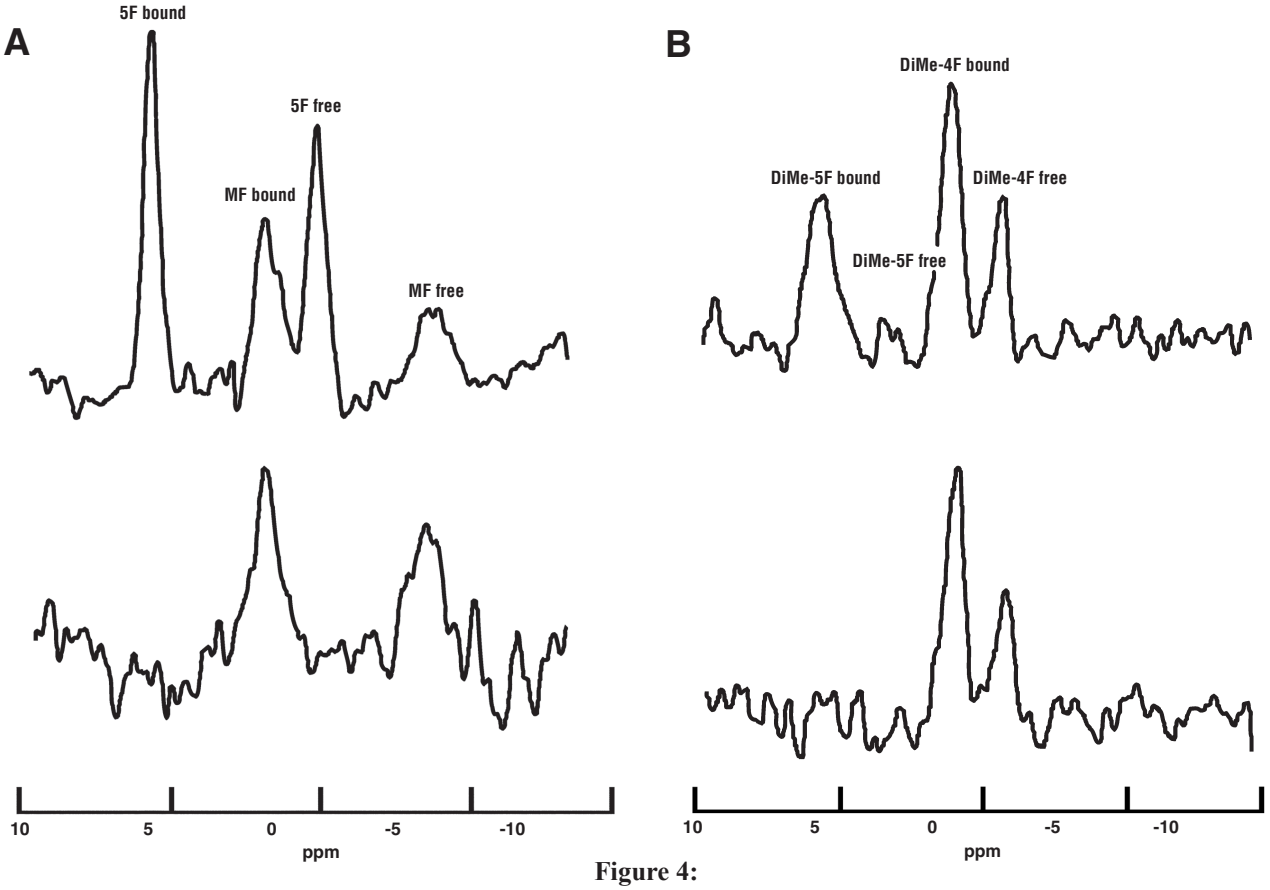

Figure 4:
(A) ^{19}FNMR spectra obtained from a Ferret heart co-loaded with 5FBAPTA after MFBAPTA.
(**B**) ^{19}FNMR spectra obtained from a Ferret heart co-loaded with DiMe-5FBAPTA after DiMe-4FBAPTA.

Discussion

The buffering effects of indicator

Ideally, the K_d of an indicator should be close to the $[Ca^{2+}]_i$ to be measured, as this will optimise sensitivity in the system [25]. With regard to ^{19}F-NMR indicators, changes in $[Ca^{2+}]_i$ near the K_d of the indicator will cause larger, and therefore more easily measurable, changes in the areas of the NMR resonances. Thus we were able to obtain measurements of end-diastolic $[Ca^{2+}]_i$ using indicators with K_d values in the range 46–2950nM at 30°C but we were only able to measure peak-systolic $[Ca^{2+}]_i$ using indicators with K_d values ≥155nM (see Table 1). These considerations suggest that 5FBAPTA (K_d, 537nM at 30°C) would be an appropriate indicator to measure both diastolic and systolic $[Ca^{2+}]_i$. However, if the cytosolic concentration of the indicator is high relative to the amount of Ca^{2+} mobilized during the Ca^{2+} transient the indicator will bind an appreciable portion of the mobilized Ca^{2+}. Hence, the change in $[Ca^{2+}]_i$ during the transient will be diminished by the added buffer, or extra calcium will be mobilised to negate this effect. The results in this study suggest that in the perfused heart the dominant effect is that the change in free $[Ca^{2+}]_i$ during the transient is reduced by the added buffer (see Table 1).

In this study all indicators were loaded to similar levels, approx. 120μM (see the Materials and methods section). Under these conditions the data show that the buffering effect of the indicators was K_d-dependent. The end-diastolic $[Ca^{2+}]_i$ was increased by the presence of an indicator and this increase was approximately

linearly related to the indicator K_d (see Figure 3A), whereas the peak-systolic $[Ca^{2+}]_i$ was reduced by the presence of the indicator with the peak-systolic $[Ca^{2+}]_i$ decreasing with decreasing indicator K_d (see Figure 3B). These empirical relationships suggested that we could use the data to extrapolate the unperturbed end-diastolic and peak-systolic $[Ca^{2+}]_i$. The extrapolations used were based on the relationships between $[Ca^{2+}]_i$ and indicator K_d as illustrated in Figure 5. The experimental data (Figure 3) show that an added buffer with a K_d in the range of the cardiac $[Ca^{2+}]_i$ transient raises end-diastolic $[Ca^{2+}]_i$ and reduces peak-systolic $[Ca^{2+}]_i$ (illustrated by the solid lines in Figure 5). If the added buffer has a very low affinity (K_d>> peak-systolic $[Ca^{2+}]_i$) it will have negligible effect on $[Ca^{2+}]_i$ because little Ca^{2+} will be bound to the indicator in either diastole or systole (broken lines in Figure 5). Conversely, if the added buffer has very high affinity (K_d<< end-diastolic $[Ca^{2+}]_i$) it will be totally bound in diastole and therefore can not bind any additional Ca^{2+} during systole and so will have negligible influence on $[Ca^{2+}]_i$. This implies that between the extremes of very high and very low K_d there must be inflexions in the measured $[Ca^{2+}]_i$ versus indicator K_d (dotted lines in Figure 5). The inflections occur on the higher affinity (low K_d) side for the systolic $[Ca^{2+}]_i$ and on the lower affinity (high K_d) side for the diastolic $[Ca^{2+}]_i$. Therefore, extrapolating to K_d=0 will give an estimate of the diastolic $[Ca^{2+}]_i$ and extrapolating to K_d=∞ will give an estimate of the systolic $[Ca^{2+}]_i$.

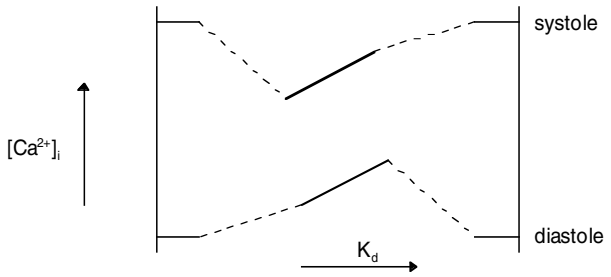

Figure 5: Diagram illustrating the effect of varying the K_d of an exogenous Ca^{2+} buffer on the Ca^{2+} transient

Indicators with very high affinity will be fully bound during both diastole and systole and so will not buffer the cardiac Ca^{2+} transient. Conversely, indicators with very low affinity will not bind Ca^{2+} during diastole or systole and so will not buffer the cardiac Ca^{2+} transient. Between these points, however, the buffering of the cardiac Ca^{2+} transient is indicator K_d dependent.

A linear function was used to extrapolate diastolic $[Ca^{2+}]_i$ and a log-linear function to extrapolate systolic $[Ca^{2+}]_i$, as these were the simplest functions that fitted the data empirically. From Figure 5 it is apparent that the extrapolations used would lead to an underestimation of the diastolic $[Ca^{2+}]_i$ and an overestimation of the systolic $[Ca^{2+}]_i$. However, the extrapolated value for the diastolic $[Ca^{2+}]_i$, 161nM, was within the error range of the diastolic $[Ca^{2+}]_i$ measured with the highest affinity indicator (171±21nM, DiMe-5FBAPTA) and the extrapolated value for systolic $[Ca^{2+}]_i$, 2650nM, was within the error range of the systolic $[Ca^{2+}]_i$ measured with the lowest affinity indicator (2510±210nM, 4,5FBAPTA). Therefore, the extrapolation function used does not appear to be a significant source of error in the estimation of the unperturbed $[Ca^{2+}]_i$ compared to the SD of 8–11% for the experimental $[Ca^{2+}]_i$ measurements. Furthermore our estimate of end-diastolic $[Ca^{2+}]_i$ agrees well with values obtained using fluorescent indicators in isolated myocytes (e.g. [26,27]) and muscle strips (e.g. [28,29]). Our estimate of peak-systolic $[Ca^{2+}]_i$ is similar to the values reported from experiments using aequorin, a low-affinity, high-sensitivity indicator, (e.g. [30]) but is higher than most values reported from experiments using fluorescent indicators. It is likely however, that the buffering properties of the fluorescent indicators means that most reported values are perturbed rather than true peak-systolic values, as has been clearly demonstrated by, for example Wier *et al.* [27], and modelled by Noble and Powell [31].

Simultaneous end-diastolic $[Ca^{2+}]_i$ measurements

From Figure 3A, it is apparent that the lower affinity indicators cause more perturbation of the diastolic $[Ca^{2+}]_i$ than higher-affinity indicators. When two indicators are loaded to similar concentrations we would therefore expect that the diastolic $[Ca^{2+}]_i$ should be closer to the value measured in the presence of the lower affinity indicator alone. The end-diastolic $[Ca^{2+}]_i$ measured by MFBAPTA was significantly increased from 324±24nM to 439±15nM following loading of a lower affinity indicator, 5FBAPTA. Similarly, the end-diastolic $[Ca^{2+}]_i$ measured by DiMe-5FBAPTA was increased from 171±21nM to 204±32nM when measured in the presence of the lower affinity indicator DiMe-4FBAPTA. In both sets of experiments the end-diastolic $[Ca^{2+}]_i$ measured by the lower affinity indicator was not significantly affected by co-loading a higher affinity indicator.

Despite the limitations of the co-loading experients, the data are consistent with the predicted effect of loading two indicators with different K_d values. Furthermore, the similarity of the $[Ca^{2+}]_i$ measured with both indicators in the co-loading experiments suggests that the relative K_d values measured by UV or NMR spectrometry *in vitro* are very similar to the relative K_d values *in vivo* and that the indicators load into the same cell compartment. The differences in end-diastolic $[Ca^{2+}]_i$ reported by the different indicators are therefore a direct result of their K_d values.

Acknowledgements

We thank Mr David Reed for excellent technical assistance. The work was supported by the Medical Research Council and a British Heart Foundation project grant. AAG is a British Heart Foundation Senior Research Fellow (FS/97026) and JIV a British Heart Foundation Basic Science Lecturer (BS/9502). MFBAPTA-AM ester was a gift from Dr R.E. London, Duke University, NC., USA.

References

1. Bers, D. (1991) Excitation contraction coupling and cardiac contractile force *Kluwer Academic Publishers, Dordrecht*
2. Blinks, J. (1991) in The Heart and Cardiovascular System (Fozzard, H., Haber, E., Jennings, R., Katz, A. and Morgan, H., eds.), pp. 1171–203, Raven Press, New York
3. Lee, H. C., Smith, N., Mohabir, R. and Clusin, W. T. (1987) Cytosolic calcium transients from the beating mammalian heart. *Proc Natl Acad Sci USA* **84**:7793–7
4. O'Rourke, B., Reibel, D. K. and Thomas, A. P. (1990) High-speed digital imaging of cytosolic Ca^{2+} and contraction in single cardiomyocytes. *Am J Physiol* **259**: H230–42
5. Spurgeon, H. A., Stern, M. D., Baartz, G., Raffaeli, S., Hansford, R. G., Talo, A., Lakatta, E. G. and Capogrossi, M. C. (1990) Simultaneous measurement of Ca^{2+}, contraction, and potential in cardiac myocytes. *Am J Physio* **258**:H574–86
6. Lorell, B. H., Apstein, C. S., Cunningham, M. J., Schoen, F. J., Weinberg, E. O., Peeters, G. A. and Barry, W. H. (1990) Contribution of endothelial cells to calcium-dependent fluorescence transients in rabbit hearts loaded with Indo-1. *Circ Ress* **67**:415–25
7. Metcalfe, J. C., Hesketh, T. R. and Smith, G. A. (1985) Free cytosolic Ca^{2+} measurements with fluorine labelled indicators using ^{19}F-NMR. *Cell Calcium* **6**:183–95
8. Kirschenlohr, H. L., Metcalfe, J. C., Morris, P. G., Rodrigo, G. C. and Smith, G. A. (1988) Ca^{2+} transient, Mg^{2+}, and pH measurements in the cardiac cycle by ^{19}F-NMR. *Proc Natl Acad Sci USA* **85**:9017–21
9. Marban, E., Kitakaze, M., Kusuoka, H., Porterfield, J. K., Yue, D. T. and Chacko, V. P. (1987) Intracellular free calcium concentration measured with ^{19}F-NMR spectroscopy in intact ferret hearts. *Proc Natl Acad Sci USA* **84**:6005–9
10. Steenbergen, C., Murphy, E., Levy, L. and London, R. E. (1987) Elevation in cytosolic free calcium concentration early in myocardial ischemia in perfused rat heart. *Circ Re* **60**:700–7
11. Smith, G. A., Hesketh, R. T., Metcalfe, J. C., Feeney, J. and Morris, P. G. (1983) Intracellular calcium measurements by ^{19}F-NMR of fluorine-labeled chelators. *Proc Natl Acad Sci USA* **80**:7178–82
12. Kirschenlohr, H., Grace, A., Shachar Hill, Y., Metcalfe, J., Morris, P. and Smith, G. (1990) Calcium measurements with a new high-affinity NMR indicator in the isolated perfused heart. *Proceedings of the Society for Magnetic Resonance in Medicine* **9**:900
13. Smith, G. and Bachelard, H. (1994) *Methods in Neuroscience* **27**:153–195
14. Song, S. K., Hotchkiss, R. S., Neil, J., Morris, P. E., Jr., Hsu, C. Y. and Ackerman, J. J. (1995) Determination of intracellular calcium in vivo via fluorine-19 nuclear magnetic resonance spectroscopy. *Am J Physiol* **269**:C318–22
15. Clarke, S., Metcalfe, J. and Smith, A. (1993) Design and properties of new ^{19}F-NMR Ca^{2+} indicators: modulation of the affinities of BAPTA derivatives *via* alkylation, *Journal of the Chemical Society-Perkin Transactions* **2**:1187–94
16. Levy, L. A., Murphy, E. and London, R. E. (1987) Synthesis and characterization of ^{19}F-NMR chelators for measurement of cytosolic free Ca. *Am J Physiol* **252**:C441–9
17. Levy, L. A., Murphy, E. and London, R. E. (1987) Synthesis and characterization of ^{19}F-NMR chelators for measurement of cytosolic free Ca. *Am J Physiol* **293**:407–11
18. Tsien, R. Y. (1981) A non-disruptive technique for loading calcium buffers and indicators into cells. *Nature* **290**:527–8
19. Martell, A. and Smith, R. (1994) *Critical Stability Constants, vol. 1,* Plenum Press, New York
20. Martell, A. and Smith, R. (1997) *Critical Stability Constants, vol. 3*, Plenum Press, New York
21. Harding, D. P., Smith, G. A., Metcalfe, J. C., Morris, P. G. and Kirschenlohr, H. L. (1993) Resting and end-diastolic $[Ca^{2+}]_i$ measurements in the Langendorff-perfused ferret heart loaded with a ^{19}F-NMR indicator. *Magn Reson Med* **29**:605–15
22. Grace, A. A., Kirschenlohr, H. L., Metcalfe, J. C., Smith, G. A., Weissberg, P. L., Cragoe, E. J., Jr. and Vandenberg, J. I. (1993) Regulation of intracellular pH in the perfused heart by external HCO_3^- and Na^+-H^+ exchange. *Am J Physiol* **265**:H289–98
23. Poenie, M., Alderton, J., Steinhardt, R. and Tsien, R. (1986) Calcium rises abruptly and briefly throughout the cell at the onset of anaphase. *Science* **233**:886–9
24. Schanne, F. A., Dowd, T. L., Gupta, R. K. and Rosen, J. F. (1989) Lead increases free Ca^{2+} concentration in cultured osteoblastic bone cells: simultaneous detection of intracellular free Pb^{2+} by ^{19}F-NMR. *Proc Natl Acad Sci USA* **86**:5133–5
25. Tsien, R. Y. (1980) New calcium indicators and buffers with high selectivity against magnesium and protons: design, synthesis, and properties of prototype structures. *Biochemistry* **19**:2396–404
26. Trafford, A. W., Diaz, M. E., O'Neill, S. C. and Eisner, D. A. (1995) Comparison of subsarcolemmal and bulk calcium concentration during spontaneous calcium release in rat ventricular myocytes. *J Physiol (Lond)* **488**:577–86
27. Balke, C. W., Egan, T. M. and Wier, W. G. (1994) Processes that remove calcium from the cytoplasm during excitation-contraction coupling in intact rat heart cells. *J Physiol (Lond)* **474**:447–62
28. Backx, P. H. and Ter Keurs, H. E. (1993) Fluorescent properties of rat cardiac trabeculae microinjected with Fura-2 salt. *Am J Physiol* **264**:H1098–110
29. Lamont, C. and Eisner, D. A. (1996) The sarcolemmal mechanisms involved in the control of diastolic intracellular calcium in isolated rat cardiac trabeculae. *Pflugers Arch* **432**: 961–9
30. Kihara, Y., Grossman, W. and Morgan, J. P. (1989) Direct measurement of changes in intracellular calcium transients during hypoxia, ischemia, and reperfusion of the intact mammalian heart. *Circ Res* **65**:1029–44
31. Noble, D. and Powell, T. (1991) The slowing of Ca^{2+} signals by Ca^{2+} indicators in cardiac muscle. *Proc R Soc Lond B Biol Sci* **246**:167–72

This page is blank

ISBN 978-0-9555321-0-8 (paperback)

ISBN: 978-0-9555321-1-5 (hardback)